Multiple sulfur isotopic evidence for the origin of elemental sulfur in an iron-dominated gas hydrate-bearing sedimentary environment

Zhiyong Lin[a,b], Xiaoming Sun[a,b,c,*], Harald Strauss[d,**], Yang Lu[a,b], Michael E. Böttcher[e], Barbara M.A. Teichert[d], Junli Gong[c], Li Xu[a,b], Jinqiang Liang[f], Hongfeng Lu[f], Jörn Peckmann[g]

[a] School of Marine Sciences, Sun Yat-sen University, Guangzhou 510006, China
[b] Guangdong Provincial Key Laboratory of Marine Resources and Coastal Engineering, Guangzhou 510006, China
[c] School of Earth Science and Engineering, Sun Yat-sen University, Guangzhou 510275, China
[d] Institut für Geologie und Paläontologie, Westfälische Wilhelms-Universität Münster, D-48149 Münster, Germany
[e] Geochemistry and Isotope Biogeochemistry Group, Marine Geology Department, Leibniz Institute for Baltic Sea Research (IOW), D-18119 Warnemünde, Germany
[f] Guangzhou Marine Geological Survey, Guangzhou 510760, China
[g] Institut für Geologie, Zentrum für Erdsystemforschung und Nachhaltigkeit, Universität Hamburg, D-20146 Hamburg, Germany

ARTICLE INFO

ABSTRACT

Elemental sulfur is commonly regarded as the product of oxidative sulfur cycling in the sediment. However, reports on the occurrence of elemental sulfur in seepage areas are few and thus its origin and mechanisms controlling its distribution are insufficiently understood. Here, we analyzed the multiple sulfur isotopic compositions for elemental sulfur and pyrite from an iron-dominated gas hydrate-bearing sedimentary environment of the South China Sea to unravel the impact of sulfate-driven anaerobic oxidation of methane (SO_4-AOM) on the formation of elemental sulfur. The multiple sulfur isotopes reveal variable ranges for both elemental sulfur and pyrite ($\delta^{34}S$: between -15.7 and $+23.3‰$ for elemental sulfur and between -35.3 and $+34.4‰$ for pyrite; $\Delta^{33}S$: between -0.08 and $+0.06‰$ for elemental sulfur and between -0.03 and $+0.15‰$ for pyrite). The enrichment of ^{34}S in pyrite throughout the sediment core suggests pronounced SO_4-AOM in paleo-sulfate-methane transition zones (SMTZ). In addition, the occurrence of seep carbonates with very negative $\delta^{13}C$ values (as low as $-57‰$, V-PDB) coincides with the inferred paleo-SMTZs and agrees with formerly locally pronounced SO_4-AOM. Interestingly, the multiple sulfur isotopic composition of elemental sulfur reveals a different pattern from that of pyrite derived from organoclastic sulfate reduction (i.e., with low $\delta^{34}S$ and high $\Delta^{33}S$ values for the latter). In comparison to coexisting pyrite, most of the elemental sulfur reveals higher $\delta^{34}S$ values (as much as $+28.9‰$), which is best explained by an enrichment of ^{34}S in the residual pool of dissolved sulfide generated by SO_4-AOM. As an intermediate sulfur phase, elemental sulfur can form via sulfide oxidation coupled to iron reduction, but it can only persist in the absence of free sulfide. Therefore, the occurrence of ^{34}S enriched elemental sulfur is likely to represent an oxidative product after hydrogen sulfide had vanished due to vertical displacement of the SMTZ. Our observations suggest that elemental sulfur may serve as a useful recorder for reconstructing the dynamics of sulfur cycling in modern and possibly ancient seepage areas.

1. Introduction

Pyritization in marine sediments contributes to a great extent to global sulfur cycling (e.g., Jørgensen, 1982; Rickard, 2012, and references therein). Organoclastic sulfate reduction (OSR) represents a key mechanism for mineralization of organic matter and sulfide production in marine sediments (Jørgensen, 1982; Canfield, 1991). Methane emissions out of the sediments are observed along continental margins worldwide (e.g., Judd et al., 2002; Johnson et al., 2003; Suess, 2014).

Sulfate-driven anaerobic oxidation of methane (Eq. (1); hereafter SO_4-AOM) has been increasingly considered as an important diagenetic process that is responsible for sulfate consumption and sulfide formation along continental margins in addition to OSR (e.g., Jørgensen et al., 2004; Reeburgh, 2007; Borowski et al., 2013; Lash, 2015; Z.Y. Lin et al., 2016a, 2016b). During SO_4-AOM, most of the upward-diffusing methane is consumed at the expense of sulfate within the sulfate-methane transition zone (SMTZ), which leads to formation of hydrogen sulfide that eventually precipitates together with iron to diagenetically

stable pyrite. It is commonly found that ^{34}S enriched authigenic sulfide is related to SO$_4$-AOM, and such enrichment has been suggested to indicate the positions of the current and/or paleo-SMTZs (e.g., Jørgensen et al., 2004; Peketi et al., 2012, 2015; Borowski et al., 2013; Q. Lin et al., 2016b; Z.Y. Lin et al., 2016a, 2016b, 2017a, 2017b).

$$CH_4 + SO_4^{2-} \rightarrow HS^- + HCO_3^- + H_2O \qquad (1)$$
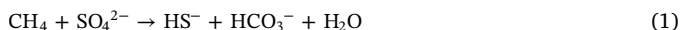
However, it is well-known that hydrogen sulfide and pyrite can be oxidized at the seabed with oxygen or even within anoxic sediments via nitrate reduction or by simultaneous reduction of metal oxides (e.g., iron oxides and manganese oxides; Thamdrup et al., 1993; Bottrell et al., 2000; Jørgensen and Nelson, 2004; Zopfi et al., 2004; Böttcher et al., 2001, 2005; Böttcher and Thamdrup, 2001; Lichtschlag et al., 2013). These processes lead to the generation of sulfate or intermediate sulfur species such as elemental sulfur (Chen and Morris, 1972; Yao and Millero, 1993, 1996; Zopfi et al., 2004; Riedinger et al., 2010). Bacterial disproportionation of elemental sulfur and other sulfur intermediates is accompanied by substantial sulfur isotope fractionation (Canfield and Thamdrup, 1994; Canfield et al., 1998; Cypionka et al., 1998; Habicht et al., 1998; Böttcher et al., 2001), which has been suggested to have a strong impact in the development of the natural sulfur isotope record (Canfield and Thamdrup, 1994; Canfield and Teske, 1996).

Although elemental sulfur is the most abundant sulfur intermediate and well documented to occur in natural surface sediments (Troelsen and Jørgensen, 1982; Thode-Andersen and Jørgensen, 1989; Anderson and Pratt, 1995; Neretin et al., 2004; Zopfi et al., 2004, 2008), its distribution in seep environments has only been reported by a few studies (Sassen et al., 2004; Lichtschlag et al., 2013; Q. Lin et al., 2015, 2016a). Lichtschlag et al. (2013) attributed the occurrence of elemental sulfur in a reduced mud volcano environment to the oxidation of hydrogen sulfide driven by iron oxides. Q. Lin et al. (2015, 2016a) noticed that significant quantities of elemental sulfur accumulate in the SMTZ and thus postulated that the formation of elemental sulfur may be related to displacement of the SMTZ. In addition, it was reported that vacuolated sulfide-oxidizing bacteria including *Beggiatoa* store elemental sulfur as internal granules during the process of sulfide oxidation in seepage environments (e.g., Sassen et al., 2004). However, direct measurements of the isotopic composition of elemental sulfur from cold-seep environments are still lacking to date, which hampers our understanding of its origin and the mechanism controlling its distribution.

In this study, we investigated the multiple sulfur isotope signatures (δ^{34}S, Δ^{33}S and Δ^{36}S) and the distribution of elemental sulfur and coexisting pyrite, as well as the carbon and oxygen isotopic compositions of seep carbonates from an iron-dominated gas hydrate-bearing sedimentary core of the northern South China Sea. The low extent of pyritization and the lower δ^{56}Fe values of pyrite than of iron oxides (Z.Y. Lin et al., 2018) observed for this core suggest that the local sedimentary environment of the Dongsha area is sulfide limited and that abundant reactive iron compounds are present. The obtained results help to better constrain how SO$_4$-AOM affects the sulfur isotopic composition of elemental sulfur and its abundance. It is documented that the occurrence of ^{34}S enriched elemental sulfur in the sediment can be used as an indicator of the location of the paleo-SMTZ, providing new insights into the dynamics of sulfur cycling in seepage areas.

2. Geological setting

The South China Sea, one of the largest marginal basins in the western Pacific Ocean, is controlled by complex interactions of the Eurasian, Pacific, and India-Australian plates (Morley, 2012). The study site is situated in the Dongsha area of the northern South China Sea (Fig. 1). The Dongsha area hosts a 10 km thick succession of sediments with complex fractures, folds, and diapirs, which favor the flow of methane-rich fluids and the formation of gas hydrates (McDonnell et al., 2000; Suess, 2005; Han et al., 2008). A wide distribution of well-

developed bottom simulating reflectors indicating the base of the gas hydrate stability zone have been recognized in this area (e.g., McDonnell et al., 2000; Suess, 2005; Wang et al., 2006; Li et al., 2015). Abundant seep carbonates were discovered along the northern slope of the South China Sea, including the *Jiulong Methane Reef*, covering about 430 km^2 (e.g., Suess, 2005; Han et al., 2008; Tong et al., 2013; Lu et al., 2015). In addition, an active cold seep with methane venting and living mussels was discovered at Site F in the Dongsha area (Feng and Chen, 2015). As one of the most promising areas for gas hydrate formation in the northern South China Sea, abundant gas hydrates were successfully drilled from the Dongsha area during China's second gas hydrate drilling expedition (GMGS-2) in 2013 (Zhang et al., 2015a). These observations confirm that seepage of methane-rich fluids and gas hydrates are common phenomena along the northern slope of the South China Sea, particularly in the Dongsha area.

3. Samples and methods

Site GMGS2-16 was drilled in the course of a drilling program during the GMGS-2 gas hydrate expedition in 2013 by the Guangzhou Marine Geological Survey (GMGS) (Fig. 1). This sampling site is among the 8 drilling sites that yielded gas hydrate (Zhang et al., 2015a). It has a water depth of 871 m and the length of the recovered core is 230 m. Gas hydrates are present in two layers of this core: (1) nodular and massive hydrates in the 15–30 mbsf interval and (2) massive hydrates in the 189–226 mbsf interval (Zhang et al., 2015a). The sediments of this core mainly consist of dark-green, unconsolidated clayey silt and silty clay. In addition, authigenic carbonate nodules with a maximal diameter of a few centimeters and fossil shells can be observed in multiple layers of this core. After retrieval, the cores were cut into sections at intervals of 70 cm from the top to the bottom, and transferred to a cold room (4 °C) for storage. Sediment samples were collected at intervals of around 5 m, packed individually in Zip-Lock plastic bags and stored frozen at −20 °C until further analysis.

In 2016, samples were dried at 40 °C in a drying oven for 24 h. An aliquot of sediment was sieved with distilled water with a 0.063 mm sieve. Authigenic carbonate, pyrite, and iron oxide aggregates were identified and hand-picked from the coarse fraction (> 0.063 mm, e.g., quartz grains, shells, authigenic minerals) under a binocular microscope. For petrographical observations, representative carbonate, pyrite, and iron oxide aggregates were examined under a Quanta 400F thermal field emission scanning electron microscope after carbon coating at the Instrumental Analysis and Research Center, Sun Yat-sen University.

For the analysis of δ^{13}C and δ^{18}O values, CO$_2$ was liberated from about 0.5 mg of carbonate powder with 100% phosphoric acid at 70 °C for 2 h and transferred into a ThermoFinnigan Gasbench II interfaced with a Delta V Advantage mass spectrometer in the School of Earth Science and Geological Engineering, Sun Yat-sen University. Stable isotope results are presented in the standard δ-notation (‰) relative to the V-PDB standard. Analytical performance was monitored by repeated analyses of the international reference material NBS-18 (δ^{13}C = −5.01‰, δ^{18}O = −23.0‰). The analytical accuracy was better than ± 0.1‰ for δ^{13}C and δ^{18}O values.

A second aliquot of dry sediment was pulverized for further sequential sulfur species extraction (cf. Canfield et al., 1986; Rice et al., 1993). Briefly, elemental sulfur (S^0) was first extracted from the sample powder by pure acetone on a rotary shaker for 18 h (Rice et al., 1993). The acetone solution was filtered and the elemental sulfur dissolved in acetone was extracted as hydrogen sulfide by reaction with 1 M CrCl$_2$ solution at sub-boiling temperatures for 2 h in an inert nitrogen atmosphere. From the remaining sediment, acid-volatile (mono)sulfide (AVS) was liberated with HCl (25%) for 1 h at room temperature, but no AVS was present in the samples. Then the samples were reacted with 1 M CrCl$_2$ solution at sub-boiling temperatures for 2 h in an inert nitrogen atmosphere for liberating chromium reducible sulfur (CRS,